OPEN

NPG Asia Materials (2013) 5, e75; doi:10.1038/am.2013.63

www.nature.com/am

REVIEW

Recent advances in the optimization and functionalization of upconversion nanomaterials for *in vivo* bioapplications

Wei Feng, Xingjun Zhu and Fuyou Li

Upconversion nanophosphors are considered to be important components in advanced materials designed for *in vivo* bioapplications and benefit from their unique anti-Stokes upconversion luminescence properties. The near-infrared light excitation allows for a large penetration depth in biotissues during *in vivo* applications. This review presents recent advances in the optimization and functionalization of upconversion nanomaterials for bioimaging and *in vivo* therapy. The most effective protocols are introduced in detail. Current limitations and future prospects are also included to provide a general summary and suggest future research directions.
NPG Asia Materials (2013) **5,** e75; doi:10.1038/am.2013.63; published online 6 December 2013

Keywords: bioimaging; *in vivo*; therapy; upconversion nanomaterials

INTRODUCTION

Upconversion luminescence (UCL) materials have attracted significant attention in recent years because of their unique ability to generate shorter wavelength emissions under longer wavelength excitations.[1] This anti-Stokes luminescence process requires the luminescent center to subsequently absorb the energy of at least two photons. The mechanism is significantly different from that of other anti-Stokes processes, such as two-photon luminescence or second harmonic generation, in which the absorption of multiple photons occurs simultaneously.

Recently, nanosized upconversion materials have been used for *in vivo* bioapplications.[2,3] Using near-infrared (NIR) radiation as an excitation source, visible or NIR emissions can be collected as signals for bioimaging. Because of the minimum absorption and scattering effects in biotissues for light in the NIR range, upconversion bioimaging is expected to have a large tissue penetration depth that is suitable for *in vivo* applications.[4,5] Currently reported results already demonstrate the ability to obtain signals at penetration depths of 3.2 cm.[6] In addition, the unique upconversion process avoids interference from the autofluorescence of biotissues because no biotissues have similar abilities to generate anti-Stokes luminescence with large Stokes shift. In addition, commonly used upconversion nanoprobes are inorganic nanocrystals that have the extremely high stability needed to ensure that the signals are steady and reliable.[7] Beyond the simple upconversion nanomaterials for bioimaging, nanocomposites containing upconversion nanophosphors (UCNPs) can also be designed to act as drug delivery containers or NIR-phototriggered devices.[8] This type of progress has greatly accelerated research into luminescence-based *in vivo* bioapplications.

To date, some researchers have already summarized the synthesis and emission color-tuning processes for the upconversion of nanoparticles and their applications in bioimaging.[3,9–15] Therefore, this review concentrates on recent advances made in the optimization and functionalization of upconversion nanomaterials for innovative *in vivo* bioapplication designs. The main discussion focuses on how the designs or protocols ensure that the upconversion nanomaterials are superior to other types of luminescent material for *in vivo* applications.

TYPICAL UPCONVERSION NANOMATERIALS

To date, the most popular upconversion nanomaterials are based on lanthanide elements that utilize abundant metastable excited states with long lifetimes as the intermediate state in the upconversion process.[1] The host lattices are usually rare earth fluorides that have low phonon energies to minimize the possibility of nonradiative transition. The most commonly used emitters are Er^{3+}, Tm^{3+} and Ho^{3+} that have main upconversion emission bands located in the green and red regions, the blue and NIR regions and the green region, respectively (Figure 1).[16] To date, the most widely investigated upconversion nanosystem is the $NaREF_4$ nanocrystal, where RE stands for rare earth elements, including Y and all the lanthanides (La to Lu). Because of the low solubility of $NaREF_4$ nanocrystals in both aqueous and organic solutions, $NaREF_4$ upconversion nanocrystals are easily synthesized using the coprecipitation method

Department of Chemistry and State Key Laboratory of Molecular Engineering of Polymers, Fudan University, Shanghai, People's Republic of China
Correspondence: Professor F Li, Department of Chemistry, Fudan University, No. 220 Handan Road, Shanghai 200433, People's Republic of China.
E-mail: fyli@fudan.edu.cn
Received 30 June 2013; revised 2 September 2013; accepted 23 September 2013

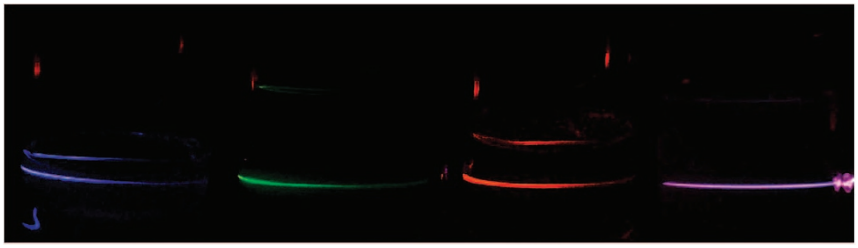

Figure 1 Typical upconversion emission photographs from upconversion nanophosphors (UCNPs) under excitation with a 980 nm laser, including $NaYbF_4$:Tm, $NaYbF_4$:Ho, $NaYbF_4$:Er and $NaYF_4$:Yb (seen from left to right). The pictures shown here are taken without optical filters and are reproduced with permission from Ehlert *et al*.[16] Copyright 2008 American Chemical Society.

from corresponding precursors to provide the required amount of elements. In addition, carrying out the coprecipitation method in high-boiling-point solvents permits more effective control over the size and shape of the products. This method is now considered the standard method for obtaining upconversion nanocrystals.[17–22] Therefore, most advances made in recent years are based on these upconversion $NaREF_4$ nanocrystals.

HIGH-EFFICIENCY UPCONVERSION NANOMATERIALS FOR *IN VIVO* BIOAPPLICATIONS

Low brightness is one of the main drawbacks of upconversion nanomaterials and limits their range during *in vivo* applications. In a typical application, a laser with a relatively high excitation power density must be used to achieve efficient UCL. For *in vivo* bioapplications in particular, a high excitation power ($>500\ mW\ cm^{-2}$) leads to a greater heating effect and increases the cost of the instruments.[23] To solve this problem, recent efforts have attempted to improve the upconversion efficiency of UCNPs by reducing the required excitation power density and improving the performance of UCNPs in bioapplications.

The low brightness of UCNPs originates from two main causes. One is the extremely low quantum efficiency. Nanosized lanthanide luminescent materials usually have much lower luminescent efficiencies than the corresponding bulk material because of large surface-to-volume ratios and poor crystallinity that produce many defects that act as quenching centers. This occurrence is an extremely important issue for UCNPs because in the upconversion process, both the intermediate excited state and the final excited state can transfer excitation energy to the quenching centers that significantly reduces the upconversion efficiency.[24] To date, the upconversion quantum efficiency of small-size UCNPs has been reported to be $<1\%$.[25,26]

To solve these problems, new materials are being designed to reduce the possibility of nonradiative transition, enhance the absorption of the sensitizers or use a combination of these methods to improve the upconversion efficiency of UCNPs.

REDUCE THE NONRADIATIVE TRANSITION POSSIBILITY

The selection of the proper host lattice can enhance the upconversion emission intensities of UCNPs. In bulk upconversion materials, hexagonal phase $NaYF_4$ is thought to be an ideal host because of its ultra-low phonon energy.[27] However, in nanoscale upconversion nanocrystals, the existence of a larger number of surface quenching centers and crystal defects originating from the small size effect enables more nonradiative transition routes that reduce the upconversion efficiency of the upconversion nanomaterials. This effect is extremely important for the UCNPs designed for *in vivo* bioapplications because small particles are necessary to enable quick excretion.

Our research group has recently reported that sub-10 nm $NaLuF_4$-based upconversion nanocrystals that are synthesized using the thermal decomposition method have higher upconversion efficiencies than corresponding $NaYF_4$-based upconversion nanocrystals obtained using the same method.[28] The absolute quantum yield of the upconversion emission centered at 800 nm for hexagonal phase $NaLu(Gd)F_4$:Yb,Tm nanocrystals ($\sim$8 nm) can reach as high as 0.47% (Figure 2). The increase in the upconversion efficiency of UCNPs also improves their *in vivo* bioimaging performance as a result of the increase in the penetration depth and detection limits.

Li and Yang and coworkers[29] reported that cubic-phase $NaLuF_4$:Yb,Tm UCNPs have higher upconversion efficiencies than $NaYF_4$:Yb,Tm UCNPs with similar dimensions (Figure 2). The as-prepared $NaLuF_4$:Yb,Tm can even be used for *in vivo* bioimaging of fur-rich mice, black mice and rabbits. In bulk materials, using $NaLuF_4$ as the host does not show obvious efficiency enhancements compared with using a $NaYF_4$ host; thus, the increase in the upconversion efficiency is mainly ascribed to the reduction in the number of surface ligands. This reduction may be the result of the different coordination abilities between the surface ligands and the various rare earth ions.

The construction of a core–shell structure is one of the most effective ways to improve the upconversion efficiency. The principle and typical structures of core–shell UCNPs designed to increase the upconversion efficiency are shown in Figure 3. Core-inert shell structures, in which the shell is the undoped host material, are designed to reduce the possibility of nonradiative transition. The introduction of an inert shell usually requires the shell material to have the same or similar lattice parameters as the core structure to minimize any lattice strains. Because there is no sensitizer or activator ion in the inert shell, the shell layer removes the energy transfer route from the activator (or sensitizer) to the surface quenching centers that reduces the possibility of nonradiative transition and increases the upconversion efficiency.

Early work in the synthesis of core–shell nanocomposites is based on the epitaxial growth of an additional shell layer with the same lattice as the core material, but without any sensitizer or activator ion. Because rare earth ions have similar properties and ionic radii, the doping of lanthanide ions causes few changes to the lattice parameters of the host material, and the inert layer can be the same as the host lattice. For example, Yan and coworkers[30] synthesized a core–shell α-$NaYF_4$:Yb,Er/Tm@α-$NaYF_4$ nanocomposite using a two-step growth method. The as-prepared α-$NaYF_4$:Yb,Er/Tm nanocrystals were used as crystallization nuclei and placed into the reaction solutions to further the growth of the inert α-$NaYF_4$ shell. Zhang and

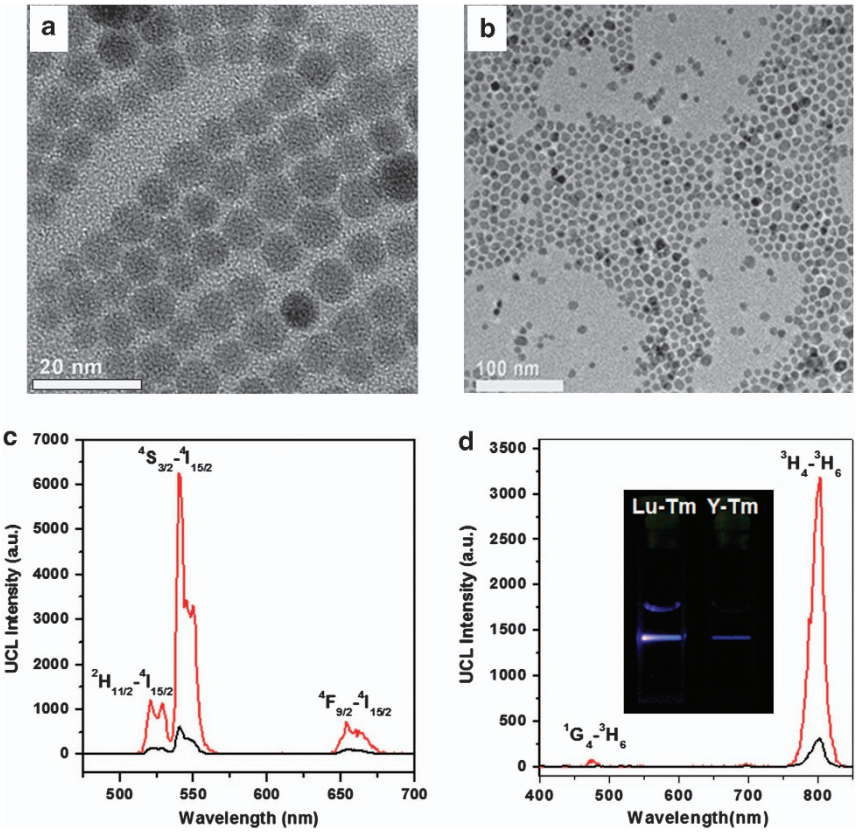

Figure 2 Transmission electron microscopy (TEM) images of (**a**) sub-10 nm β-phase $NaLuF_4$:24%Gd,20%Yb,2%Er (Lu) and (**b**) sub-20 nm α-phase $NaLuF_4$:20%Yb,2%Er; also shown are the upconversion luminescence (UCL) spectra of (**c**) Lu, (red line), $NaYF_4$: 20%Yb,2%Er (Y, black line), (**d**) $NaLuF_4$:24%Gd,20%Yb,2%Tm (Lu–Tm, red line), and $NaYF_4$: 20%Yb, 1%Tm (Y–Tm black line). The inset shows a photograph of the UCL emission of Lu–Tm and Y–Tm. Reprinted with permission from Liu *et al.*[26] and Yang *et al.*[29] Copyright 2011 American Chemical Society. Copyright 2012 Elsevier B.V.

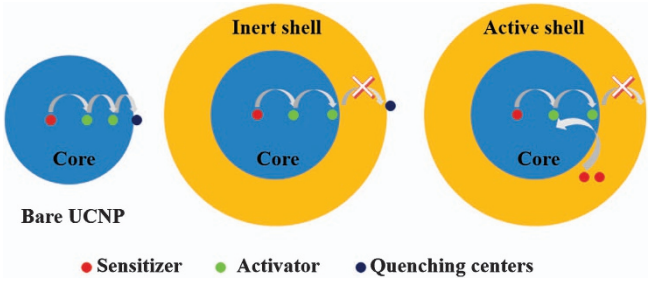

Figure 3 The design and structures of core–shell upconversion nanocomposites for improving upconversion efficiencies. UCNP, upconversion nanophosphor.

coworkers[31] also fabricated core–shell β-$NaYF_4$:Yb,Er/Tm@β-$NaYF_4$ nanocomposites to improve the upconversion efficiency. This method is widely used and has been extended to similar upconversion systems, such as rare earth fluorides,[30,32] oxides[33] and oxyfluorides.[34] In addition, Zhang and Zhao and coworkers[35] controlled the addition of the precursors in the shell layer to precisely control the thickness of the shell with an accuracy at a monolayer level. Furthermore, they investigated the relationship between the thickness of the shell layer and the upconversion emission intensities. An electron energy loss spectroscopy mapping technique was employed at low temperatures to characterize the shell thickness and to avoid any damage originating from electron collisions.

Recently, van Veggel and coworkers[36] demonstrated a new protocol to synthesize core–shell structures. Using α-$NaYF_4$ nanocrystals as precursors, β-$NaYF_4$ shells were grown on the surfaces of β-$NaYF_4$:Yb,Er nanocrystals (core) layer by layer via a recrystallization process. The thickness of the shell layer can be controlled by adjusting the initial ratio of α-$NaYF_4$ to β-$NaYF_4$:Yb,Er in the reaction solution.

In addition to the growth of a shell with the same lattice as the host of core material, other inorganic host materials with similar lattice parameters are also used to construct core–shell upconversion nanocomposites. Recently, Yan and coworkers[37] developed a CaF_2-coated upconversion nanocomposite for improving the UCL efficiency. Because CaF_2 has nearly the same lattice parameter as the cubic $NaYF_4$ host, it is possible to precisely control the epitaxial growth process to obtain the desired thickness in the shell layer. The core–shell structure is easily characterized in a high-angle annular dark-field image because of the wide difference between the atomic numbers of Y and Ca. The upconversion emission intensity can be enhanced by ~300 times in $NaYF_4$:Yb,Er@CaF_2. Furthermore, the CaF_2 shell hinders the effective release of rare earth ions into the biosurroundings, reducing the possible toxicity of UCNPs (Figure 4).

ENHANCE THE ABSORPTION ABILITY

Another reason for the low upconversion efficiency in UCNPs is the low absorption cross-section of the lanthanide ions. The absorption cross-section of Yb^{3+}, a commonly used sensitizer, is much lower than for organic dyes, quantum dots or noble metal nanocrystals.[38]

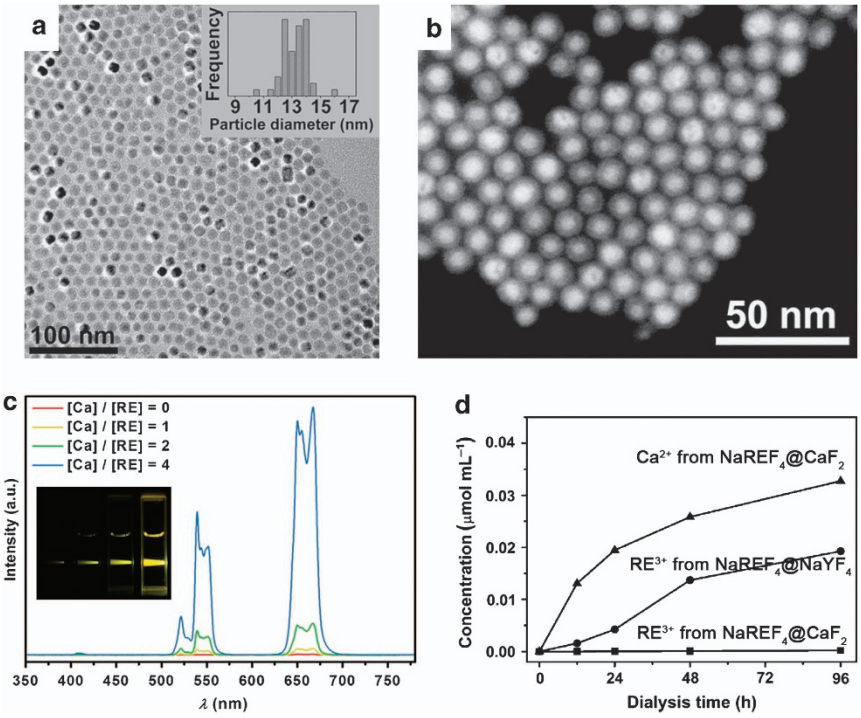

Figure 4 (**a**) Transmission electron microscopy (TEM) image, (**b**) HAADF image and (**c**) upconversion emission spectra of the core–shell $NaYF_4$:Yb,Er@CaF_2 nanocomposites with different Ca/RE (RE = Y + Yb + Er) ratios; (**d**) the released concentration of rare earth or Ca^{2+} ions from different upconversion nanostructures, indicating the suppressed RE^{3+} leakage upon coating of the CaF_2 shell. Reproduced with permission from Wang *et al*.[37] Copyright 2012 Wiley-VCH Verlag GmbH & Co. KGaA, Weinheim.

Therefore, the absorption efficiency of UCNPs is lower than for the conventional fluorescence process.

To solve this problem, an active shell has recently been designed for upconversion nanocomposites to increase the upconversion efficiency by doping the sensitizer Yb^{3+} ions in the shell layer. The additional sensitizer ions increase the possibility to absorb excitation photons, improving the UCL.

For example, to absorb more excitation photons at 980 nm, Capobianco and coworkers[39] fabricated a core–shell $NaGdF_4$:Yb,Er@-$NaGdF_4$:Yb nanocomposite by introducing an active shell containing an appropriate amount of Yb^{3+} ions. Some other core-active shell nanostructures, such as $BaGdF_5$:Yb,Er@$BaGdF_5$:Yb[40] and @$NaYF_4$:Yb,Er@$NaYF_4$:Yb,[41] have also been fabricated to enhance the upconversion emission intensities. In these core–shell structured UCNPs, the amount of Yb^{3+} in the active shell needs to be optimized because the Yb^{3+} can also provide a route to transfer the absorbed excitation energy to the surface quenching centers, which weakens the upconversion emission.

Another route for increasing the absorption of NIR light is by utilizing a well-known metal surface-enhanced fluorescence phenomenon. It has been proven that incident electric fields redistribute on the surface of metal nanocrystals because of the existence of surface plasmons in metals. The intensity of the electric field can be enhanced by several orders of magnitude in this way at some hot spots. Commonly used metals include Gold (Au) and Silver (Ag) for the surface plasmon resonance bands located in the visible range. Early studies have proven that the upconversion emissions from Er^{3+} in solid-state films are enhanced in the presence of Ag nanocrystals.[42] Yan and coworkers[43] reported that the upconversion emissions from $NaYF_4$:Yb,Er nanocrystals are also enhanced in the presence of Ag nanowires, which proves it is possible to construct nanocomposites with noble metals to enhance the upconversion emission intensity. Duan and coworkers[44] demonstrated enhancements to the UCL of $NaYF_4$:Yb,Tm nanocrystals by absorbing Au nanocrystals through electrostatic interactions with the assistance of polyelectrolytes. The emission intensity was enhanced by up to 150% with the proper amount of Au nanoparticles. In addition, a series of similar upconversion nanocomposites with noble metals has been fabricated to enhance the upconversion emissions.[45–49] Unfortunately, most of this work focuses on observing the enhancement effects rather than describing the detailed mechanism behind them. Therefore, there is no confirmed information available to direct the design of such nanocomposites to further improve the upconversion emissions until now.

The third and newest route to enhance the absorption abilities of UCNPs is to use a NIR organic dye as an energy absorber. Although organic dyes have larger absorption cross-sections than commonly used sensitizer Yb^{3+} ions, it is difficult to use a sensitizer to increase the UCL because of the lack of fundamental studies on the energy transfer process from organic dyes to rare earth ions. Recently, Hummelen and coworkers[50] proved the feasibility of using a NIR dye to increase the absorption of excitation light. A commercial cyanine dye, IR-780, was selected as the antenna molecule. After carboxylic acid functionalization, the IR-780 bound to the surface of a $NaYF_4$:Yb,Er nanocrystal (UCNPs) instead of the original oleylamine through a ligand exchange process. The resulting nanocomposite had an enhanced upconversion emission that is ~1100 times stronger than that of the original oleylamine-coated UCNPs and broadened the excitation peaks to permit the utilization of more excitation light. This experimental result is important because it enables the use of organic dyes to sensitize lanthanide upconversion nanophosphors.

UCNPs BASED ON TRIPLET–TRIPLET ANNIHILATION

Another type of UCNP using a triplet–triplet annihilation (TTA) upconversion process has recently been employed for *in vivo* bioapplications using organic molecules as sensitizers. For this upconversion mechanism, the sensitizer and emitter are both organic molecules, and the triplet state of these organic molecules is used as the intermediate state in the upconversion process.[51] TTA-based UCL processes benefit from the high absorption cross-section of organic dyes and the highly efficient TTA process between emitter molecules that usually have much stronger absorption and higher UCL efficiencies than lanthanide-based UCL processes. To date, the highest quantum efficiency reported for TTA-based UCL processes exceeds 40%,[52] and some systems have proven to be functional under excitation from only sunlight.[51]

The problem limiting bioapplications of TTA-based upconversion materials is that the TTA process needs to occur in a medium with proper liquidity to ensure opportunities for collisions between the emitters and sensitizers so that energy transfer takes place. Therefore, TTA-based materials cannot be used for *in vivo* bioapplications until a suitable assembly method is developed to obtain upconversion nanoparticles with fluxible, or at least flexible, media inside. Recently, we reported a silica coating method to wrap the sensitizer and emitter molecules together in an inorganic structure with the assistance of polyethyleneglycol F127 (Figure 5).[53] The as-prepared 10 nm silica nanospheres, containing 2,7,8,12,13,17,18-octaethylporphyrin palladium (PdOEP) and 9,10-diphenylanthracene (DPA) molecules (as shown in Figure 5), were used as sensitizers and emitters, respectively. These nanospheres could be used as upconversion nanoprobes for *in vivo* bioimaging experiments despite the upconversion emission located in the blue spectral region when they were subjected to a 532 nm laser excitation. This was the first demonstration of TTA-based UCNPs being used for *in vivo* bioimaging of the whole body of a small animal. The excitation power density can decrease to 8.5 mW cm^{-2} because the PdOEP sensitizer has a large absorption cross-section. The quantum yield of these TTA UCNPs reached 4.5% (for an excitation power density of 260 mW cm^{-2}) in an aqueous solution.

Furthermore, we developed a nanocapsule strategy to load TTA-based UCL systems into nanoparticles.[54] The nanocapsules were composed of an oil droplet and a surface bovine serum albumin–dextran layer to protect the oil phase. The TTA sensitizer and emitter molecules were easily loaded into the oil droplets without significantly affecting their mobility and luminescence properties. The high solubility of the sensitizer and emitter molecules in the oil droplets also suppressed possible aggregation-induced quenching of the luminescence. By using platinum(II) tetraphenyltetrabenzoporphyrin (PtTPBP) and boron-dipyrromethene (BODIPY)-based molecules as the sensitizer and emitter (Figure 5), respectively, the quantum yield of the nanocapsule reached 4.8% in an aqueous solution. Because the development of TTA-based upconversion nanocomposites is still in the initial stages, we only provide these examples here. The following chapters will still focus on lanthanide-based upconversion nanomaterials.

SURFACE MODIFICATION OF UCNPs FOR BIOCOMPATIBILITY

UCNPs for *in vivo* bioapplications must have biocompatible surface properties. Because the majority of high-efficiency and uniform UCNPs are synthesized in organic solvents by the thermal decomposition method or the modified solvothermal method, the surfaces of these UCNPs are capped by hydrophobic organic ligands that hinder the dispersion of UCNPs in biocompatible aqueous solutions.[17–20] To date, various methods have been developed to modify the surface of UCNPs and are summarized in the published reviews.[3] Almost all types of functional bioimaging applications employing UCNPs use surface modification methods to introduce the required surface ligands to improve biocompatibility.

Silica coatings are generally used to provide biocompatibility to hydrophobic UCNPs. Reverse micelle-based silica coating is a well-developed method for coating a silica layer on hydrophobic UCNPs.[19] Because this method is well investigated and reviewed, it is not discussed in detail here. Alternatively, we focus on a recently developed ligand exchange procedure that is a convenient and effective method for modifying the surface of hydrophobic UNCPs.

In particular, three methods have recently been developed to synthesize organic ligand-free UCNPs. Capobianco and coworkers[55] used HCl to acidify a solution containing OA (oleic acid)-capped UCNPs. OA molecules can be protonated when the pH of the solution is adjusted to a particular value that greatly weakens the coordination ability of the OA molecules to the rare earth ions. Thus, the OA ligands are replaced by other counter-ions, and the hydrophobic UCNPs become hydrophilic. Murray and coworkers[56] developed $NOBF_4$ as an agent to remove the original capping ligand on the hydrophobic UCNPs. The ion NO^+ can replace surface rare earth ions and coordination ligands. The as-prepared UCNPs are hydrophilic, with NO^+ on the surface and BF_4^- as the counter-ion (Figure 6). Our group reported a similar protocol using Gd^{3+} as cations instead of NO^+ to replace the surface rare earth ions and form a 'naked' surface.[57]

Importantly, the interaction between surface rare earth ions and the introduced counter-ions is quite weak; thus, the counter-ions are easily replaced by other additional, functional ligands with good coordination abilities with respect to rare earth ions. Therefore, the so-called ligand-free state is available to bind to the following ligands as required, and this method can be used as a general protocol for the surface modification of OA-capped UCNPs.

Although these ligand exchange protocols have been proven to effectively modify the surface of UCNPs, the detailed state of the newly introduced surface ligands is not clear after the upconversion materials are injected into small animals and needs to be explored in future research.

After causing the hydrophobic UCNPs to become hydrophilic, further surface modifications are applied to prolong the circulation time of the UCNPs in the blood. Typically, after intravenous injection, the UCNPs can only perform simple imaging on the liver, spleen or lungs, through which the UCNPs are filtered or captured by the macrophage system of the animal. Various efforts have been undertaken to solve this problem, and polyethylene glycol (PEG) is now regarded as the most effective surface ligand to prolong the circulation time of UCNPs in blood by suppressing the capture of UCNPs by the macrophage system. The PEG moieties can be introduced onto UCNPs by using amino- or COOH-modified PEG species or by using some amphiphilic polymers containing PEG chains directly. Liu and coworkers[58] investigated the long-term biodistribution of UCNPs with different surface modification species. Compared with the polyacrylic acid-modified UCNPs, PEG-coated UCNPs have longer blood circulation half-lives. This result proves that PEG reduces the nonspecific interactions of UCNPs with the macrophage system and delays uptake by macrophages.

UPCONVERSION NANOMATERIALS AS FUNCTIONAL INDICATORS FOR BIOIMAGING

Recent developments in upconversion nanomaterial research have focused on the design and fabrication of upconversion probes for

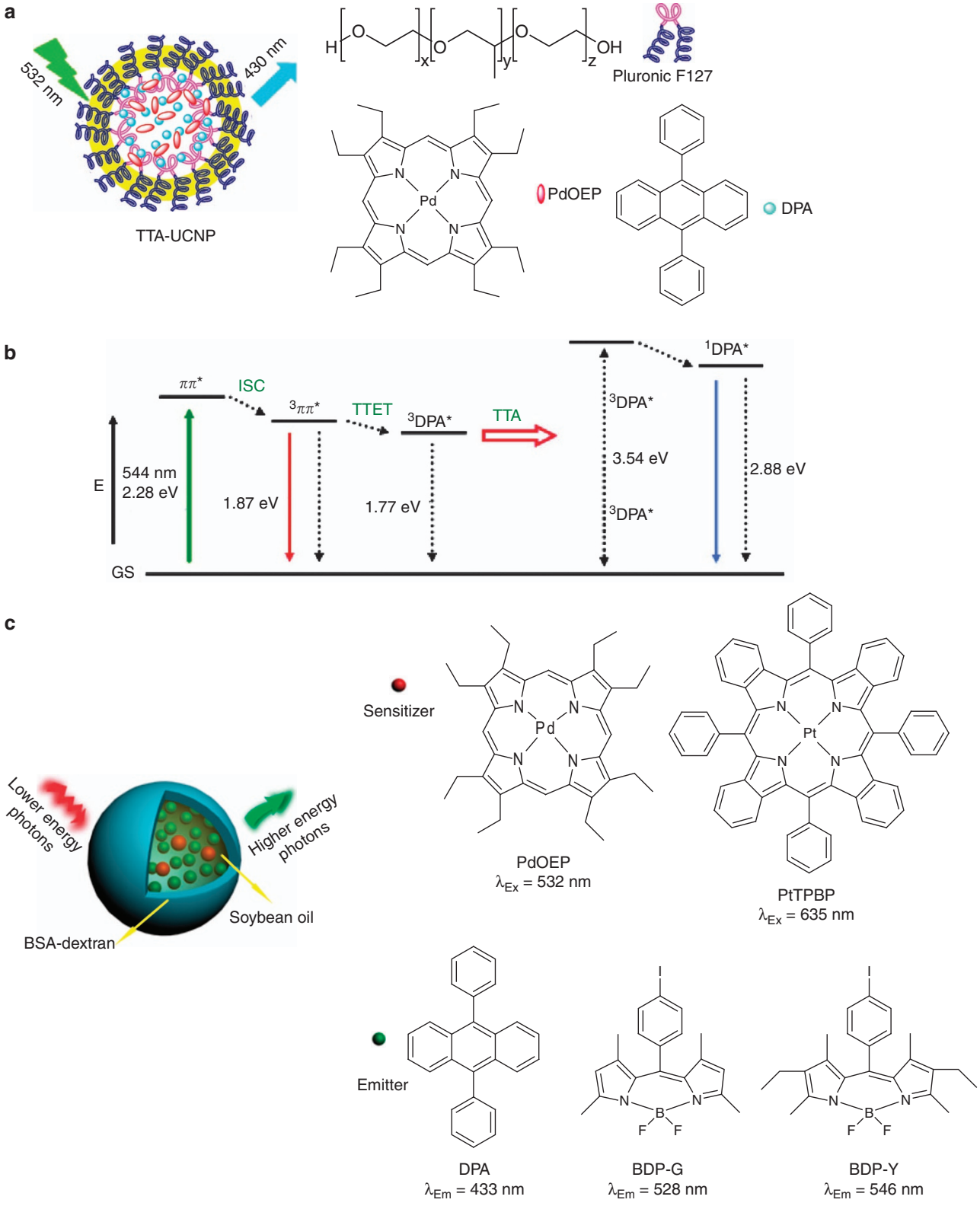

Figure 5 (**a**) The structure of the hydrophilic triplet–triplet annihilation upconversion nanophosphor (TTA-UCNP) based on silica coating in which the yellow ring represents the silica shell; (**b**) a schematic illustration of the corresponding upconversion mechanism based on the TTA process and (**c**) the structure of the bovine serum albumin (BSA)–dextran-based TTA-UCNP, sensitizers and emitters. Reproduced with permission from Liu *et al.*[53,54] Copyright 2010 American Chemical Society.

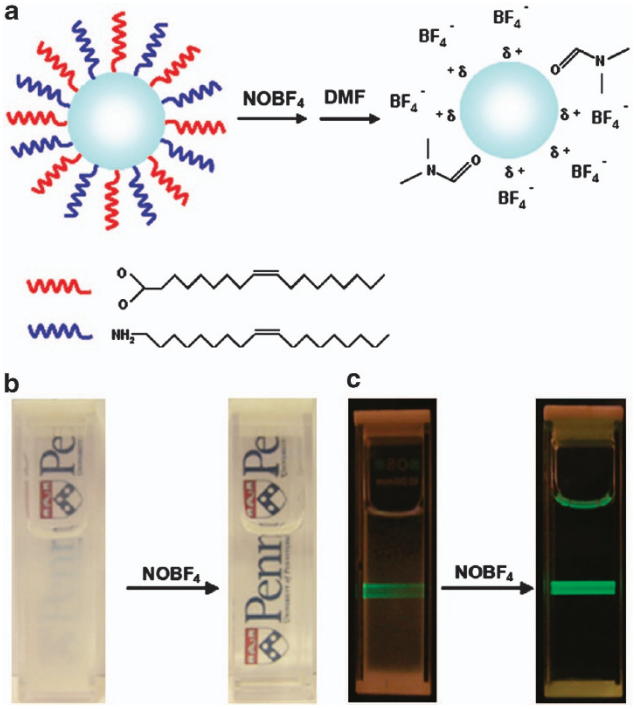

Figure 6 (**a**) Schematic illustration of the preparation procedure to produce ligand-free upconversion nanophosphors (UCNPs) with the assistance of $NOBF_4$, (**b**) the improved colloidal stability and (**c**) the upconversion efficiency after treatment. Reproduced with permission from Dong *et al*.[56] Copyright 2010 American Chemical Society.

functional bioimaging. To date, upconversion probes have been successfully designed for cell tracking and for *in vivo* monitoring of the lymph nodes, tumors and specific analytes. Multimodality bioimaging probes have also been designed for colocalization of the probes.

UCNPs FOR LYMPH BIOIMAGING

The lymphatic system holds a very important place in the tumor metastasis process, but it is difficult to study the lymphatic system because of the shortage of imaging techniques with proper sensitivity and temporal–spatial resolution. UCNPs are ideal fluorescence probes used for *in vivo* lymph imaging because the probes injected into the paw of a mouse can easily reach the sentinel lymph nodes through lymphatic vessels and exhibit intense UCL signals.[59,60] Recently, TTA-based UCNPs have also been successfully used for *in vivo* lymph imaging. Our group has used silica-coated PdOEP and DPA nanoparticles with blue upconversion emission (excited at 532 nm) for the imaging of lymph nodes in living mice.[53] Because the detection signal from the blue upconversion emission becomes poor as the penetration depth increases, imaging can only be obtained after removal of the skin of the mice. If another TTA-based UCNP composed of PtTPBP and BDP, oil and bovine serum albumin–dextran possessing a green (or yellow) upconversion emission (excited at 635 nm) is used as the probe, then lymphatic images can be easily obtained *in vivo* and without removal of the skin.[54]

UCNPs DESIGNED FOR TUMOR-TARGETED IMAGING

In addition to basic imaging of the liver or spleen by simply injecting the hydrophilic UCNPs into the mouse via the tail vein, researchers also want to utilize UCNPs for functional imaging experiments. Tumor targeting is one of the most attractive functional imaging applications because of the importance of tumor detection and in-clinic therapy.

Some studies have reported that the enhanced permeability and retention effect of tumors can cause nanosized probes to concentrate in the tumor site. However, the targeting efficiency is relatively low for UCNPs, and additional functionalization is needed for more accurate targeting. Folic acid, peptides and antibodies are the most commonly used targeting groups to help nanoparticles find tumor sites.

Our group has reported using folic acid-modified $NaYF_4$:Yb,Er (FA-UCNPs) for *in vivo* tumor target imaging.[61] Folic acid is joined with the amino group containing UCNPs to target tumor cells with a folic receptor. After intravenous injection of FA-UCNPs into a HeLa tumor-bearing athymic nude mouse for 24 h, a red upconversion emission was detected at the tumor site. Our group also used an Arg-Gly-Asp (RGD) tripeptide to target $\alpha_v\beta_3$-overexpressing U87MG tumors.[62] To accomplish this, RGD tripeptide was covalently bonded to PEG-NH_2-modified $NaYF_4$:Yb,Tm nanocrystals (RGD-UCNPs). The 800 nm upconversion emission of RGD-UCNPs was detected at tumor sites, reaching a maximum emission 4 h after intravenous injection of the UCNPs into a U87MG tumor-bearing mouse.

In addition, antibodies can be joined to the UCNPs for targeted imaging of tumor cells, based on the antibody–antigen interaction. For example, Xu, Mao and coworkers[63] linked rabbit anti-CEA8 antibodies to silica-coated $NaYF_4$:Yb,Er UCNPs with $-NH_2$ groups to target a carcinoembryonic antigen in HeLa cells. However, thus far there has been no mention in the literature of tumor imaging at the animal level using UCNPs designed to focus on the antibody–antigen interaction.

UCNPs FOR MONITORING ANALYTES *IN VIVO*

UCNPs can be used for upconversion detection in a nanosystem composed of UCNPs and chemodosimeters with an efficient energy transfer process. If this nanosystem is introduced into animals, the detection of upconversion may be used to monitor the concentration of analytes *in vivo*.

Very recently, our group employed a hydrophobic heptamethine cyanine dye (hCy7) as a $MeHg^+$-responsive chemodosimeter to combine with UCNPs to detect $MeHg^+$ *in vivo*.[64] An amphiphilic polymer (P-PEG) was used to coat the $NaYF_4$:Yb,Er,Tm UCNP to provide a hydrophobic layer to load hCy7 and a hydrophilic layer to endow the nanocomposite with biocompatibility. The absorption of the hCy7 corresponded to an upconversion emission at 660 nm from Er^{3+} so that efficient energy transfer would occur to stop any green upconversion emissions in the initial state. After the addition of $MeHg^+$, the hCy7 reacted with $MeHg^+$ and changed to hCy7', and the absorption band redshifted to 845 nm. This matched the upconversion emission at 800 nm from Tm^{3+}. The ratio of the upconversion emission intensity at 660 nm to that at 800 nm can be used as a detection signal to monitor the concentration of $MeHg^+$. Because of the high penetration depth of the radiation at 800 nm, these nanocomposites were further applied to monitor the presence of $MeHg^+$ in the liver of a living mouse for *in vivo* upconversion detection (Figure 7). Although this is the first example of *in vivo* upconversion detection at the animal level, the concept and protocol shown in this report are broad and can be used to construct similar systems to monitor other functional species *in vivo*, thus providing information about the analytes in a more direct and timely manner.

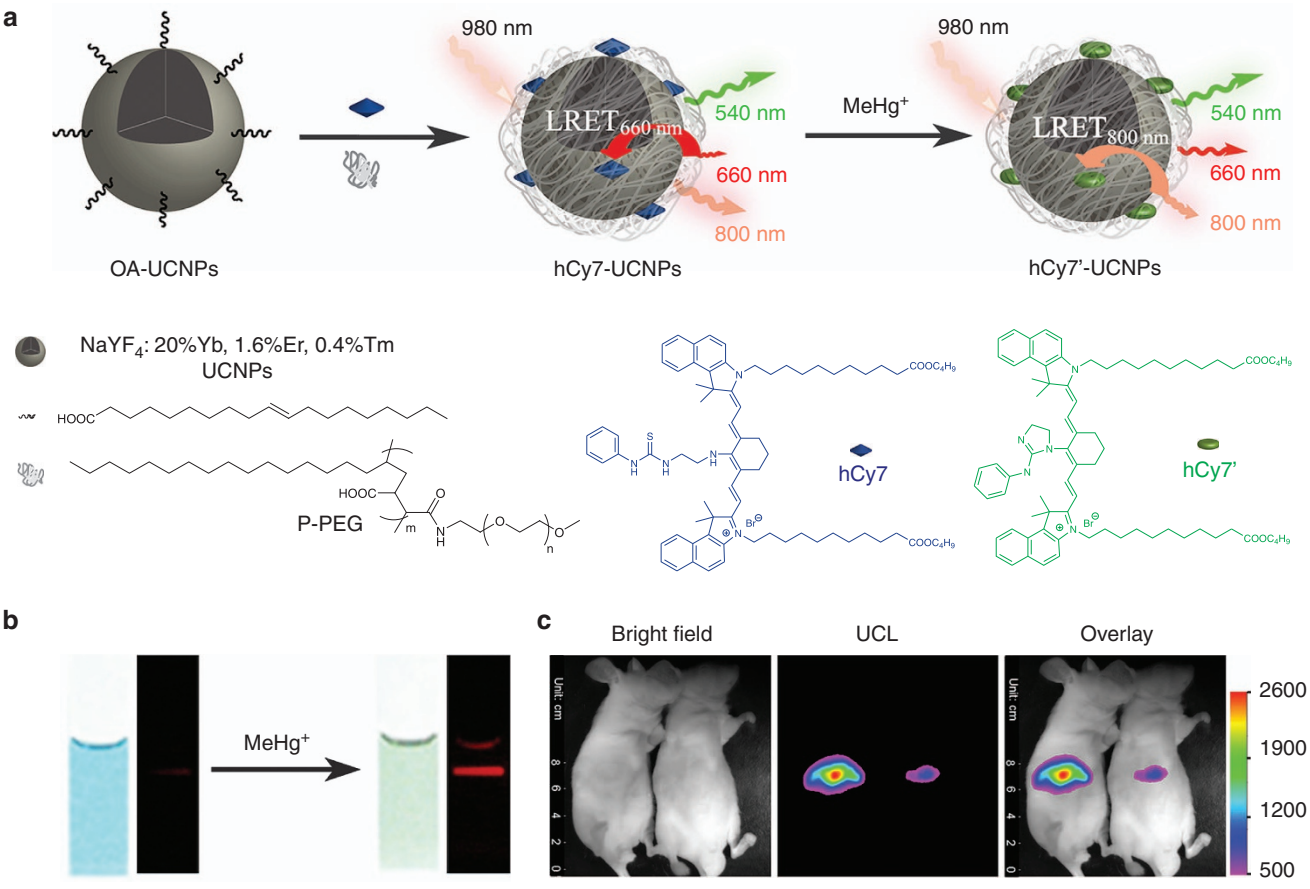

Figure 7 (**a**) Schematic design of the upconversion probes for *in vivo* monitoring of $MeHg^+$, (**b**) the detection of $MeHg^+$ in solution and (**c**) a mouse. Reproduced with permission from Liu *et al.*[64] Copyright 2013 American Chemical Society.

UCNPs FOR CELL TRACKING

Another bioimaging application of UCNPs is cell tracking. After incubation with UCNPs, specific cells can be stained by the UCNPs and exhibit upconversion emissions during their activity in the biosystem. Because of the ultra-high photostability of UCNPs, cell tracking using UCNPs as probes is expected to allow longer-term tracking of cells than what is presently accomplished with commercial dyes. For example, Liu and coworkers[65] used $NaY_{0.78}Yb_{0.2}Er_{0.02}F_4$, $NaY_{0.69}Yb_{0.3}Er_{0.01}F_4$ and $NaY_{0.78}Yb_{0.2}Tm_{0.02}F_4$ nanocrystals with different emission wavelengths to label mouth epidermal carcinoma (KB) cells for cell tracking. KB cells labeled by UCNPs with different emission wavelengths were injected into different sites of a nude mouse. At 1 week after injection, the upconversion emissions from three types of UCNPs were detectable in the three different tumor sites, as expected, that demonstrates the cell tracking ability of UCNPs (Figure 8).

Our group also reported on core–shell structured $NaYF_4$:Yb,Er,Tm@$NaLuF_4$ UCNPs with bright upconversion emissions that can be used for cell tracking.[66] The UCNP-labeled JEG-3 cells were then injected intravenously into a nude mouse. Tumors were detected in the lung, and the upconversion emission signal illustrated the ongoing metastasis process. This upconversion signal was still detectable 21 days after the injection. Recently, UCNPs have also been used to track stem cells. Liu and coworkers[67] used a PEG-conjugated Au-Fe_3O_4-UCNP nanocomposite to label marrow mesenchymal stem cells taken from Balb/C mice. The magnetic field induced accumulation of the labeled stem cells in the wound site, proving the potential of the upconversion imaging technique to guide the concentration of stem cells. Han and coworkers[68] also reported the labeling of rat mesenchymal stem cells and tracked the labeled stem cells to determine their osteogenic and adipogenic behaviors.

The upconversion materials used for cell tracking have no specific requirements, but effective cell staining and high photostability must be achieved without hindering the biological activities of the cell.

MULTIMODALITY IMAGING

Another type of upconversion nanomaterial attracting a great deal of attention for *in vivo* bioimaging is the multimodality probe. Multimodality images not only confirm the upconversion imaging results but also combine the advantages of multiple types of imaging modes that bridge gaps in sensitivity, resolution and penetration depth for multilevel molecular imaging from the cellular scale to the whole body. To date, upconversion nanoprobes have been successfully designed for integration with commercial medical imaging devices, such as magnetic resonance imaging, X-ray computer tomography, positron emission tomography (PET) and single-photon emission computed tomography (SPECT).

Typically, the T_1-enhanced magnetic resonance imaging ability is provided by Gd^{3+} doped into the lattice or joined to the surface of UCNPs.[69,70] The T_2-enhanced magnetic resonance imaging is usually provided by Fe_3O_4 components integrated with the UCNPs.[71,72] X-ray computer tomography imaging contrast is achieved by using the rare

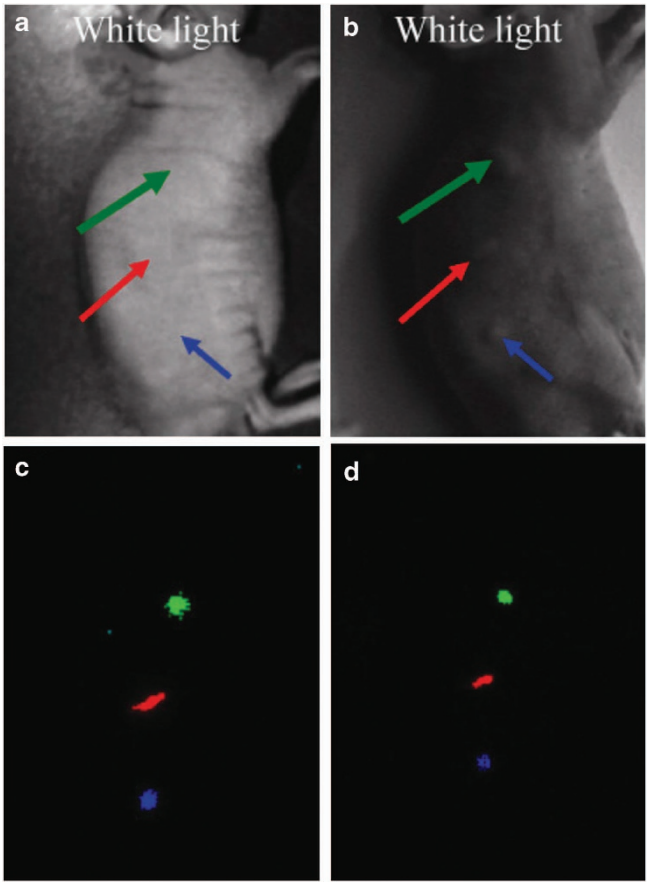

Figure 8 Multicolor *in vivo* cancer cell tracking and imaging with different upconversion nanophosphors (UCNPs). The upper images are (**a**) white light photos of a nude mouse after subcutaneous injection of the UCNP-labeled KB cells and (**b**) the same mouse after 1 week with visible tumor tissues. The lower images (**c**, **d**) are the corresponding false color upconversion luminescence images. Reproduced with permission from Cheng *et al*.[65] Copyright 2010 The Authors.

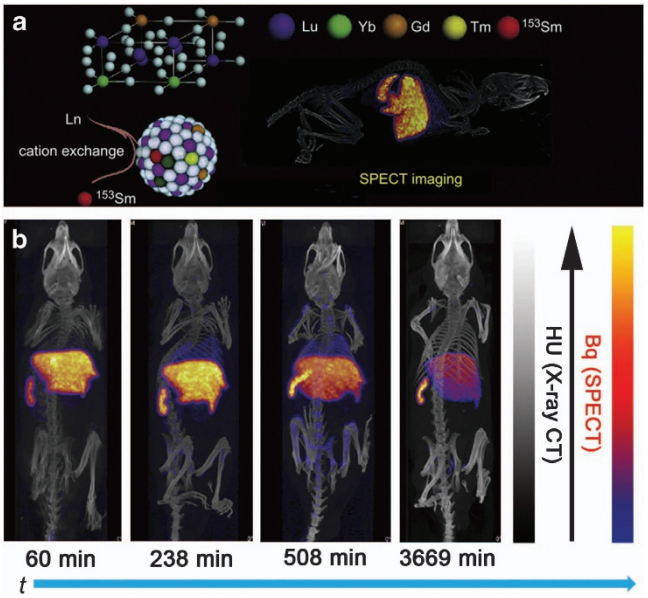

Figure 9 (**a**) The design and structure of the nanoparticles used to integrate radioactive ^{153}Sm into the lattice of the upconversion nanophosphors (UCNPs) and (**b**) an *in vivo* single-photon emission computed tomography (SPECT) image of a mouse obtained at different times after intravenous injection of ^{153}Sm-labeled UCNPs. Reproduced with permission from Sun *et al*.[75] Copyright 2012, Elsevier Ltd.

earth elements themselves[73] or by introducing a commercial contrast agent.[74]

Recently, PET and SPECT imaging functionality has also been developed for UCNPs. This development is especially useful for *in vivo* tracking of UCNPs and for providing useful information for biodistribution studies of these nanoprobes. Our group reported an ^{18}F labeling method to integrate PET imaging ability into UCNPs.[57] Because of the strong interaction between F and rare earth elements, $^{18}F^-$ cations were easily bonded to the surface of UCNPs by simply mixing the solution containing $^{18}F^-$ and UCNPs. After the $^{18}F^-$ labeled UCNPs were injected into the paw of a mouse, the PET imaging signal could be detected in the lymph node. Because of the high sensitivity of the PET imaging technique, this PET–UCL dual modality imaging can also be used to monitor the biodistribution of UCNPs. However, the radiative half-life of $^{18}F^-$ is only 2 h, which is too short to monitor the long-term biodistribution of UCNPs. SPECT imaging provides a robust technique for long-term observation of the probes by utilizing ^{153}Sm as the radioactive isotope with a half-life as long as 46.3 h.

Our group also developed a cation exchange method to introduce ^{153}Sm into the lattice of UCNPs to replace the original rare earth ions.[75] The labeling procedure is fast and convenient and is based on simply mixing a solution containing $^{153}Sm^{3+}$ and UCNPs. The ^{153}Sm-labeled UCNPs can then be used to investigate the long-term *in vivo* biodistribution of UCNPs. For example, the redistribution process of UCNPs from the liver to the spleen after intravenous injection can be clearly observed in SPECT images (Figure 9). Moreover, by taking advantage of the long half-life, ^{153}Sm can also be doped into the lattice of UCNPs during the synthesis procedure.[76] The long-term biodistribution of ^{153}Sm-labeled UCNPs has been successfully studied using quantitative SPECT imaging.

Because these multimodality contrast agents can be integrated into a nanocomposite to achieve *in vivo* multimodality imaging, the combination of different imaging techniques can be easily achieved to provide *in vivo* images with high accuracy, sensitivity and spatial resolution.

UPCONVERSION NANOMATERIALS FOR THERAPY

In addition to imaging applications, UCNPs have recently been introduced as important components in advanced nanocomposites designed for therapy. In these nanocomposites, UCNPs can be used as radiation sources to convert the wavelength of incident light to make functional components work under NIR excitation or as luminescent indicators to help locate the position or monitor the state of nanocomposites for therapy.

UCNPs AS NIR INDICATORS FOR PHOTOTHERMAL THERAPY

UCNPs are widely used to trace other drugs for therapy by simply integrating the drugs and UCNPs together without any interaction. In this type of nanostructure, UCNPs are only used to trace the drugs by relying on their UCL emissions. For example, photothermal therapy (PTT) is a recently developed and convenient method to kill cancer cells using heating caused by the absorption of the incident light. During the therapy process, PTT drugs only need to remain at the tumor site to absorb the incident light and do not need to be released

as chemotherapy drugs. Therefore, the UCNPs integrated with the PTT drugs only need to indicate the position of the nanostructure.

Au and Ag nanoparticles with surface plasmon resonance absorption in the visible to NIR regions are the most common PTT drugs. Song and coworkers[77] synthesized core–shell structured $NaYF_4$:Yb,Er@Ag for therapeutic applications. Ag nanocrystals were grown on the surface of UCNPs with the assistance of thiol groups grafted onto the UCNPs. The as-prepared nanostructures could then be used for upconversion cell imaging. The cancer cells incubated with the $NaYF_4$:Yb,Er@Ag were killed by applying 808 nm laser radiation to heat the cells. Liu and coworkers[78] also reported on a nanostructure that combined PTT drugs and UCNPs. An Au shell was chosen as the PTT drug to be grown outside the $NaYF_4$:Yb,Er nanocrystal with the assistance of an Fe_3O_4 intermediate layer. The nanocomposites were heated by absorbing 808 nm incident radiation, and the $NaYF_4$:Yb,Er provided UCL signals. The intermediate Fe_3O_4 layer endowed the nanostructures with magnetic resonance imaging contrast abilities as well as the potential to be manipulated by an external magnetic field.

UCNPs AS NIR INDICATORS FOR DRUG DELIVERY

Chemotherapy drugs often need to be loaded into a drug delivery system to control the release of drugs or to protect them before reaching the afflicted region. In a drug delivery system, UCNPs can first be used as simple luminescent indicators to help locate the position of the nanocomposites. The simplest system utilizes silica-coated UCNPs that have upconversion properties and a suitable cavity in the silica layer to load the drugs. Drugs can be loaded into the nanocavity by simple physical adsorption or by hydrophobic-hydrophobic interactions inside the porous silica layer. For example, Lin and coworkers[79] coated a mesoporous silica layer onto β-$NaYF_4$:Yb,Er nanocrystals to load drug molecules. The mesoporous structure of the silica layer provided a large cavity volume to increase the loading capacity of the upconversion nanocomposite. The upconversion emission was used to track the distribution of the drug carriers.

Furthermore, UCNPs can be used as indicators to monitor the release of drugs in the delivery system based on the energy transfer process. Lin and coworkers[80] loaded ibuprofen molecules into core–shell structured multifunctional Fe_3O_4@SiO_2@m-SiO_2@$NaYF_4$:Yb,Er nanocomposites. The magnetic core allowed the drug carrier to be manipulated by a external magnetic field. Because of the spectral overlap between the absorption of the ibuprofen molecules and the green upconversion emission of $NaYF_4$:Yb,Er, the effective energy transfer reduced the green upconversion emission intensity. Along with the release of ibuprofen drugs, the green upconversion emissions were detected and used as a signal for monitoring the quantity of drugs released.

Another recently developed nanostructure for drug delivery uses a yolk-shell silica layer outside the upconversion nanocrystal.[81] The cavity of the yolk-shell silica layer is much larger than the common mesoporous silica layer and allows the opportunity to load more drugs into the nanocomposites.

UCNPs AS NIR PHOTOTRIGGERS FOR DRUG DELIVERY

In these drug delivery nanocomposites, drug molecules can only be released by the diffusion resulting from a concentration gradient that cannot be controlled during the metabolism process. Recently, phototrigger systems have been used to allow the remote-controlled release of drugs. The physical or chemical properties of the phototrigger system are modified by absorbing radiation of a specific wavelength. If a change in properties can lead to the release of drugs, then a controllable drug carrier system can be constructed. Conventional phototrigger systems work under ultraviolet (UV) or visible light excitation that cannot be used to control drug release because of their absorption by skin and biotissues. UCNPs allow the use of low-power NIR radiation, which possesses a large penetration depth, as the excitation radiation for phototrigger systems.

Branda and Zhao and coworkers[82] reported on an upconversion phototriggered micelle system composed of poly(ethylene oxide)-block-poly(4,5-dimethoxy-2-nitrobenzyl methacrylate) and $NaYF_4$:Yb,Tm@$NaYF_4$ UCNPs. The mechanism behind this system involves UCNPs converting the 980 nm excitation radiation to UV upconversion emissions and transferring the energy to the *o*-nitrobenzyl group on the micelle core-forming block that induces a photo-cleavage reaction and destroys the micelle structure. A hydrophobic compound, Nile Red, can be used as the model for drug molecules to be loaded inside the micelle. Under 980 nm laser radiation, the micelle was broken to release Nile Red, proving the viability of this NIR-triggered drug release system.

The photo-induced isomerization of azobenzene can also be used as a phototrigger switch to control the release of drugs at a cellular level.[83] In a recently reported example, the anticancer drug doxorubicin was loaded in the mesoporous silica coating on $NaYF_4$:Yb,Tm@$NaYF_4$. Azobenzene groups were covalently bonded to the walls in the mesoporous silica shell. Under NIR excitation, the UCNPs generated visible and UV emissions to drive the isomerization of azobenzene. The corresponding wagging motion acted as a molecular impeller to help release the drug molecules (Figure 10).

Subsequent research has been performed on a similar structure for *in vivo* applications. Xing and coworkers[84] demonstrated use of the 1-(2-nitrophenyl)ethyl group as a phototrigger to control the release of molecular model D-luciferin. The photo-caged D-luciferin molecules were covalently bonded to the surface of $NaYF_4$:Yb,Tm@$NaYF_4$@SiO_2 nanoparticles. Under irradiation from a 980 nm laser, UCNPs generated upconversion emissions at 365 nm and transferred energy to the 1-(2-nitrophenyl)ethyl group to release the D-luciferin molecules. The NIR radiation-driven photorelease of D-luciferin has been demonstrated in MCF-7 cells and living mice.

Because of the excellent tissue penetration depth of NIR light and high UCL energy, phototrigger systems have successfully been used with NIR light to control the delivery of small interfering RNA both *in vitro* and *in vivo*.[85,86] As a result of UV emissions from UCNPs generated by 980 nm light exposure, the small interfering RNA loaded on the UCNPs can be released at similar levels of bioactivity by silencing the gene expression in a cell or even in deep tissue.

Different types of drug delivery systems can be fabricated with UCNPs. Future research will be carried out to enable the controllable, precise release of drugs via the upconversion process. The phototrigger groups are key factors that need to be explored to increase the quantum efficiency.

UCNPs AS WAVELENGTH CONVERTER FOR PHOTODYNAMIC THERAPY (PDT)

Another typical therapeutic use for UCNP-based nanosystems involves employing UCNPs as wavelength converters to enable a commercial PDT agent to be activated under NIR excitation. Generally, commercial PDT drugs are excited by UV or visible light to generate reactive oxygen species and kill the target cells. The poor penetration ability of UV and visible light limits the application of current PDT drugs to the treatment of superficial diseases. The integration of UCNPs and PDT drugs utilizes the unique upconversion process to modify the NIR excitation light to UV or visible emissions. The subsequent energy transfer process from the UCNP to

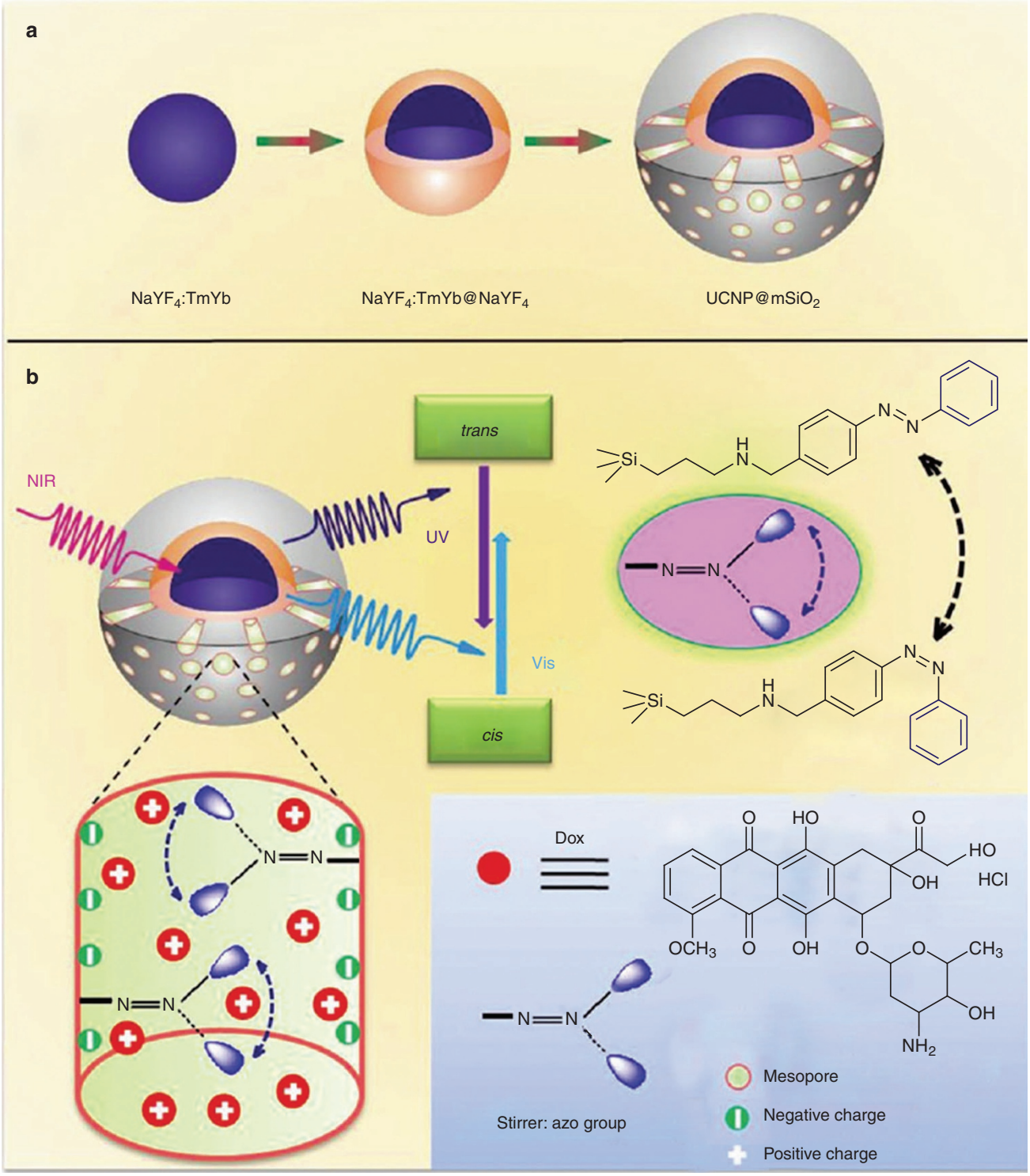

Figure 10 (**a**) An illustration of the structure of the near-infrared (NIR)-triggered drug delivery system and (**b**) the drug release mechanism driven by NIR irradiation. Reproduced with permission from Liu *et al*.[83] Copyright 2013 Wiley-VCH Verlag GmbH & Co. KGaA, Weinheim.

the PDT drugs generates reactive oxygen species and activates PDT drugs (Figure 11).[87] PDT drugs can be loaded by adsorption in the mesoporous silica layer that is coated onto UCNP surfaces to effectively receive energy from UCNPs.[88] Further research is needed to covalently bond PDT drugs to the silica layer to permit more stable PDT drugs to function in the NIR range.[32,89]

All of these nanosystems have proven to have significant therapeutic effects at both the cellular and animal levels. For example, Zhang and coworkers[90] loaded photosensitizer merocyanine 540 (MC540) and zinc(II) phthalocyanine (ZnPc) into a mesoporous silica layer that was coated onto $NaYF_4$:Yb,Er nanocrystals. The UCNPs generated green and red upconversion emissions to

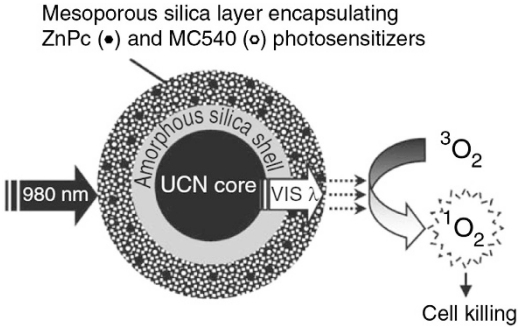

Figure 11 Schematic illustration of the upconversion nanostructure used to load drugs for near-infrared (NIR)-triggered photodynamic therapy using an energy transfer process. Reproduced with permission from Idris *et al.*[90] Copyright 2013 Wiley-VCH Verlag GmbH & Co. KGaA, Weinheim.

stimulate MC540 and ZnPc, respectively, to produce singlet oxygen and destroy nearby cells. The dual PDT approach based on excitation by a single wavelength laser is more effective than using a PDT agent. Liu and coworkers[91] developed a simple strategy to load the PDT agent chlorin e6 (Ce6) directly into the hydrophobic layer outside UCNPs and subsequently coat an amphiphilic polymer outside the UCNPs to make them water dispersible. The as-prepared nanocomposites achieved effective NIR light-induced PDT in the animal experiment. Hyeon and coworkers[92] also reported similar nanocomposite with Ce6 covalently bonded to amine-functionalized UCNPs for PDT applications. More recently, Liu and coworkers[93] constructed a charge-reversible nanocomposite with pH-sensitive surface properties containing Ce6 for better PDT performance against acidic tumors.

CONCLUSIONS AND FUTURE PROSPECTS

The advantages of UCNPs make them useful for *in vivo* bioapplications. Rapid developments in this area have proven that UCNPs can be used as luminescent probes with high penetration depths, the absence of autofluorescence and high photostability for bioimaging. In addition to other functional components, UCNPs in nanocomposites exhibit wavelength conversion abilities. Because of the small size of UCNPs and the unique UCL process, most of the potential future applications of UCNPs are still based on *in vivo* bioapplications, where their advantages can be fully utilized. However, there are still several problems that need to be solved before clinical experiments can be initiated.

First, the luminescent efficiency of UCNPs is still low, and lasers need to be used as the excitation source for the imaging process and for other applications. The high power density of lasers leads to possible tissue damage and causes heating effects. The core–shell structure currently functions well to improve the quantum efficiency. However, the low absorption cross-section of the sensitizer Yb^{3+} still poses a major problem for future research and limits the utilization of excitation light. Some protocols discussed here attempt to solve this problem, but none have exhibited sufficient improvement to make UCNPs operational at low excitation energy densities ($\sim 10\,mW\,cm^{-2}$). Organic dye-sensitized lanthanide upconversion nanosystems seem to provide a potential route to reduce the required excitation energy density, but the detailed mechanism and upconversion efficiencies need to be further investigated. Moreover, the photostability of such a nanocomposite also becomes problematic because of the introduction of organic NIR dyes.

Recently, TTA-based upconversion materials have been reported for bioprobes as an alternative to lanthanide upconversion phosphors.[53,54] Because of their relatively high absorption coefficient and upconversion efficiency, these TTA-based upconversion materials can be excited by low-power density radiation. However, the synthesis of such TTA-based upconversion nanomaterials through NIR emissions, as well as related issues such as long-term stability, biodistribution and toxicity, still need to be addressed.

Second, the relatively strong absorption of 980 nm light by water causes noticeable overheating effects. Improving the upconversion efficiency certainly reduces the required excitation power density and thus suppresses the effects of overheating. However, new efforts have been recently undertaken to design new structures to solve this problem. For example, Zhan and coworkers[23] reported using a 915 nm laser as an excitation source to achieve *in vivo* bioimaging with lower overheating effects. More recently, Nd^{3+} ions have been introduced as antenna to absorb the excitation light and further transfer energy to Yb^{3+} ions to sensitize activators to generate UCL at excitations of 808 nm.[94–96] This new strategy has been proven to mitigate overheating effects.

The third problem is the possible toxicity of UCNPs. To date, only a few reports have considered the biodistribution and possible excretion of UCNPs. The current data show that most UCNPs accumulate in the liver and spleen after injection and require a very long time to be cleared. Further research needs to focus on this issue to determine the possible applications for UCNPs. If UCNPs do not cause long-term effects in animals, they can be used directly by injection into the blood circulation system. Otherwise, they can only be used for applications in conjunction with a proven method to clear the UCNPs from the body. Once these concerns are addressed, UCNPs are destined for use in a new generation of probes for a wide range of *in vivo* applications.

ACKNOWLEDGEMENTS

We thank the National Science Foundation of China (21231004, 21201038), MOST of China (2011AA03A407 and 2012CB932403) and Shanghai Sci. Tech. Comm. (12JC1401300) for their financial support.

1 Auzel, F. Upconversion and anti-stokes processes with f and d ions in solids. *Chem. Rev.* **104,** 139–173 (2004).
2 Chatterjee, D. K., Gnanasammandhan, M. K. & Zhang, Y. Small upconverting fluorescent nanoparticles for biomedical applications. *Small* **6,** 2781–2795 (2010).
3 Zhou, J., Liu, Z. & Li, F. Y. Upconversion nanophosphors for small-animal imaging. *Chem. Soc. Rev.* **41,** 1323–1349 (2012).
4 Nyk, M., Kumar, R., Ohulchanskyy, T. Y., Bergey, E. J. & Prasad, P. N. High contrast in vitro and in vivo photoluminescence bioimaging using near infrared to near infrared up-conversion in Tm^{3+} and Yb^{3+} doped fluoride nanophosphors. *Nano Lett.* **8,** 3834–3838 (2008).
5 Pichaandi, J., Boyer, J. C., Delaney, K. R. & van Veggel, F. C. J. M. Two-photon upconversion laser (scanning and wide-field) microscopy using Ln^{3+}-doped $NaYF_4$ upconverting nanocrystals: a critical evaluation of their performance and potential in bioimaging. *J. Phys. Chem. C* **115,** 19054–19064 (2011).
6 Chen, G. Y., Shen, J., Ohulchanskyy, T. Y., Patel, N. J., Kutikov, A., Li, Z. P., Song, J., Pandey, R. K., Ågren, H., Prasad, P. N. & Han, G. (α-$NaYbF_4$:Tm^{3+})/CaF_2 core/shell nanoparticles with efficient near-infrared to near-infrared upconversion for high-contrast deep tissue bioimaging. *ACS Nano* **6,** 8280–8287 (2012).
7 Liu, Q., Feng, W., Yang, T. S., Yi, T. & Li, F. Y. Upconversion luminescence imaging of cells and small animals. *Nat. Protoc.* **8,** 2033–2044 (2013).
8 Feng, W., Han, C. M. & Li, F. Y. Upconversion-nanophosphor-based functional nanocomposites. *Adv. Mater.* **25,** 5287–5303 (2013).
9 Haase, M. & Schäfer, H. Upconverting nanoparticles. *Angew. Chem. Int. Ed.* **50,** 5808–5829 (2011).
10 Wang, F., Banerjee, D., Liu, Y. S., Chen, X. Y. & Liu, X. G. Upconversion nanoparticles in biological labeling, imaging, and therapy. *Analyst* **135,** 1839–1854 (2010).
11 Mader, H. S., Kele, P., Saleh, S. M. & Wolfbeis, O. S. Upconverting luminescent nanoparticles for use in bioconjugation and bioimaging. *Curr. Opin. Chem. Biol.* **14,** 582–596 (2010).

12 Hilderbrand, S. A. & Weissleder, R. Near-infrared fluorescence: application to in vivo molecular imaging. *Curr. Opin. Chem. Biol.* **14,** 71–79 (2010).
13 Xu, C. T., Zhan, Q. Q., Liu, H. C., Somesfalean, G., Qian, J., He, S. L. & Andersson-Engels, S. Upconverting nanoparticles for pre-clinical diffuse optical imaging, microscopy and sensing: current trends and future challenges. *Laser Photonics Rev.* **7,** 663–697 (2013).
14 Gorris, H. H. & Wolfbeis, O. S. Photon-upconverting nanoparticles for optical encoding and multiplexing of cells, biomolecules, and microspheres. *Angew. Chem. Int. Ed.* **52,** 3584–3600 (2013).
15 Gnach, A. & Bednarkiewicz, A. Lanthanide-doped up-converting nanoparticles: merits and challenges. *Nano Today* **7,** 532–563 (2012).
16 Ehlert, O., Thomann, R., Darbandi, M. & Nann, T. A four-color colloidal multiplexing nanoparticle system. *ACS Nano* **2,** 120–124 (2008).
17 Mai, H. X., Zhang, Y. W., Si, R., Yan, Z. G., Sun, L. D., You, L. P. & Yan, C. H. High-quality sodium rare-earth fluoride nanocrystals: controlled synthesis and optical properties. *J. Am. Chem. Soc.* **128,** 6426–6436 (2006).
18 Boyer, J. C., Vetrone, F., Cuccia, L. A. & Capobianco, J. A. Synthesis of colloidal upconverting $NaYF_4$ nanocrystals doped with Er^{3+}, Yb^{3+} and Tm^{3+}, Yb^{3+} via thermal decomposition of lanthanide trifluoroacetate precursors. *J. Am. Chem. Soc.* **128,** 7444–7445 (2006).
19 Jalil, R. A. & Zhang, Y. Biocompatibility of silica coated $NaYF_4$ upconversion fluorescent nanocrystals. *Biomaterials* **29,** 4122–4128 (2008).
20 Yi, G. S. & Chow, G. M. Synthesis of hexagonal-phase $NaYF_4$:Yb,Er and $NaYF_4$:Yb,Tm nanocrystals with efficient up-conversion fluorescence. *Adv. Funct. Mater.* **16,** 2324–2329 (2006).
21 Zeng, J. H., Su, J., Li, Z. H., Yan, R. X. & Li, Y. D. Synthesis and upconversion luminescence of hexagonal-phase $NaYF_4$:Yb, Er, phosphors of controlled size and morphology. *Adv. Mater.* **17,** 2119–2123 (2005).
22 Wang, G. F., Peng, Q. & Li, Y. D. Lanthanide-doped nanocrystals: synthesis, optical-magnetic properties, and applications. *Acc. Chem. Res.* **44,** 322–332 (2011).
23 Zhan, Q. Q., Qian, J., Liang, H. J., Somesfalean, G., Wang, D., He, S. L., Zhang, Z. G. & Andersson-Engels, S. Using 915 nm laser excited $Tm^{3+}/Er^{3+}/Ho^{3+}$-doped $NaYbF_4$ upconversion nanoparticles for in vitro and deeper in vivo bioimaging without overheating irradiation. *ACS Nano* **5,** 3744–3757 (2011).
24 Wang, F., Wang, J. & Liu, X. G. Direct evidence of a surface quenching effect on size-dependent luminescence of upconversion nanoparticles. *Angew. Chem. Int. Ed.* **49,** 7456–7460 (2010).
25 Boyer, J. C. & van Veggel, F. C. J. M. Absolute quantum yield measurements of colloidal $NaYF_4$:Er^{3+},Yb^{3+} upconverting nanoparticles. *Nanoscale* **2,** 1417–1419 (2010).
26 Liu, Q., Sun, Y., Yang, T. S., Feng, W., Li, C. G. & Li, F. Y. Sub-10 nm hexagonal lanthanide-doped $NaLuF_4$ upconversion nanocyrstals for sensitive bioimaging in vivo. *J. Am. Chem. Soc.* **133,** 17122–17125 (2011).
27 Krämer, K. W., Biner, D., Frei, G., Güdel, H. U., Hehlen, M. P. & Lüthi, S. R. Hexagonal sodium yttrium fluoride based green and blue emitting upconversion phosphors. *Chem. Mater.* **16,** 1244–1251 (2004).
28 Liu, Q., Sun, Y., Yang, T., Feng, W., Li, C. & Li, F. Sub-10 nm hexagonal lanthanide-doped $NaLuF_4$ upconversion nanocrystals for sensitive bioimaging in vivo. *J. Am. Chem. Soc.* **133,** 17122–17125 (2011).
29 Yang, T. S., Sun, Y., Liu, Q., Feng, W., Yang, P. Y. & Li, F. Y. Cubic sub-20 nm $NaLuF_4$-based upconversion nanophosphors for high-contrast bioimaging in different animal species. *Biomaterials* **33,** 3733–3742 (2012).
30 Mai, H. X., Zhang, Y. W., Sun, L. D. & Yan, C. H. Highly efficient multicolor up-conversion emissions and their mechanisms of monodisperse $NaYF_4$:Yb,Er core and core/shell-structured nanocrystals. *J. Phys. Chem. C* **111,** 13721–13729 (2007).
31 Wang, Y., Tu, L. P., Zhao, J. W., Sun, Y. J., Kong, X. G. & Zhang, H. Upconversion luminescence of beta-$NaYF_4$:Yb^{3+},Er^{3+}@beta-$NaYF_4$ core/shell nanoparticles: excitation power, density and surface dependence. *J. Phys. Chem. C* **113,** 7164–7169 (2009).
32 Zhao, Z. X., Han, Y. N., Lin, C. H., Hu, D., Wang, F., Chen, X. L., Chen, Z. & Zheng, N. F. Multifunctional core–shell upconverting nanoparticles for imaging and photodynamic therapy of liver cancer cells. *Chem. Asian J.* **7,** 830–837 (2012).
33 Zhang, F., Haushalter, R. C., Haushalter, R. W., Shi, Y. F., Zhang, Y. C., Ding, K. L., Zhao, D. Y. & Stucky, G. D. Rare-earth upconverting nanobarcodes for multiplexed biological detection. *Small.* **7,** 1972–1976 (2011).
34 Yi, G. S., Peng, Y. F. & Gao, Z. Q. Strong red-emitting near-infrared-to-visible upconversion fluorescent nanoparticles. *Chem. Mater.* **23,** 2729–2734 (2011).
35 Zhang, F., Che, R. C., Li, X. M., Yao, C., Yang, J. P., Shen, D. K., Hu, P., Li, W. & Zhao, D. Y. Direct imaging the upconversion nanocrystal core/shell structure at the subnanometer level: shell thickness dependence in upconverting optical properties. *Nano Lett.* **12,** 2852–2858 (2012).
36 Johnson, N. J., Korinek, A., Dong, C. & van Veggel, F. C. J. M. Self-focusing by ostwald ripening: a strategy for layer-by-layer epitaxial growth on upconverting nanocrystals. *J. Am. Chem. Soc.* **134,** 11068–11071 (2012).
37 Wang, Y. F., Sun, L. D., Xiao, J. W., Feng, W., Zhou, J. C., Shen, J. & Yan, C. H. Rare-Earth nanoparticles with enhanced upconversion emission and suppressed rare-Earth-ion leakage. *Chem. Eur. J.* **18,** 5558–5564 (2012).
38 Li, S. F., Zhang, M., Peng, Y., Zhang, Q. Y. & Zhao, M. S. Rate equation model analysis on the infrared and upconversion emission of Er/Yb co-doped borate-silicate glass. *J. Rare Earths* **28,** 237–242 (2010).
39 Vetrone, F., Naccache, R., Mahalingam, V., Morgan, C. G. & Capobianco, J. A. The active-core/active-shell approach: a strategy to enhance the upconversion luminescence in lanthanide-doped nanoparticles. *Adv. Funct. Mater.* **19,** 2924–2929 (2009).
40 Yang, D. M., Li, C. X., Li, G. G., Shang, M. M., Kang, X. J. & Lin, J. Colloidal synthesis and remarkable enhancement of the upconversion luminescence of $BaGdF_5$:Yb^{3+}/Er^{3+} nanoparticles by active-shell modification. *J. Mater. Chem.* **21,** 5923–5927 (2011).
41 Liu, X. M., Kong, X. G., Zhang, Y. L., Tu, L. P., Wang, Y., Zeng, Q. H., Li, C. G., Shi, Z. & Zhang, H. Breakthrough in concentration quenching threshold of upconversion luminescence via spatial separation of the emitter doping area for bio-applications. *Chem. Commun.* **47,** 11957 (2011).
42 Mertens, H. & Polman, A. Plasmon-enhanced erbium luminescence. *Appl. Phys. Lett.* **89,** 211107 (2006).
43 Feng, W., Sun, L. D. & Yan, C. H. Ag nanowires enhanced upconversion emission of $NaYF_4$:Yb,Er nanocrystals via a direct assembly method. *Chem. Commun.* **29,** 4393–4395 (2009).
44 Zhang, H., Li, Y. J., Ivanov, I. A., Qu, Y. Q., Huang, Y. & Duan, X. F. Plasmonic modulation of the upconversion fluorescence in $NaYF_4$:Yb/Tm hexaplate nanocrystals using gold nanoparticles or nanoshells. *Angew. Chem. Int. Ed.* **49,** 2865–2868 (2010).
45 Schietinger, S., Aichele, T., Wang, H. Q., Nann, T. & Benson, O. Plasmon-enhanced upconversion in single $NaYF_4$:Yb^{3+}/Er^{3+} codoped nanocrystals. *Nano Lett.* **10,** 134–138 (2010).
46 Liu, N., Qin, W. P., Qin, G. S., Jiang, T. & Zhao, D. Highly plasmon-enhanced upconversion emissions from Au@beta-NaYF4:Yb,Tm hybrid nanostructures. *Chem. Commun.* **47,** 7671–7673 (2011).
47 Yuan, P. Y., Lee, Y. H., Gnanasammandhan, M. K., Guan, Z. P., Zhang, Y. & Xu, Q. H. Plasmon enhanced upconversion luminescence of $NaYF_4$:Yb, Er@SiO_2@Ag core-shell nanocomposites for cell imaging. *Nanoscale* **4,** 5132–5137 (2012).
48 Zhang, F., Braun, G. B., Shi, Y. F., Zhang, Y. C., Sun, X. H., Reich, N. O., Zhao, D. Y. & Stucky, G. Fabrication of Ag@SiO_2@Y_2O_3:Er nanostructures for bioimaging: tuning of the upconversion fluorescence with silver nanoparticles. *J. Am. Chem. Soc.* **132,** 2850–2851 (2010).
49 Fujii, M., Nakano, T., Imakita, K. & Hayashi, S. Upconversion luminescence of Er and Yb codoped $NaYF_4$ nanoparticles with metal shells. *J. Phys. Chem. C* **117,** 1113–1120 (2013).
50 Zou, W. Q., Visser, C., Maduro, J. A., Pshenichnikov, M. S. & Hummelen, J. C. Broadband dye-sensitized upconversion of near-infrared light. *Nat. Photonics* **6,** 560–564 (2012).
51 Singh-Rachford, T. N. & Castellano, F. N. Photon upconversion based on sensitized triplet-triplet annihilation. *Coordin. Chem. Rev.* **254,** 2560–2573 (2010).
52 Cheng, Y. Y., Fückel, B., Khoury, T., Clady, R. G. C. R., Tayebjee, M. J. Y., Ekins-Daukes, N. J., Crossley, M. J. & Schmidt, T. W. Kinetic analysis of photochemical upconversion by triplet −triplet annihilation: beyond any spin statistical limit. *J. Phys. Chem. Lett.* **1,** 1795–1799 (2010).
53 Liu, Q., Yang, T. S., Feng, W. & Li, F. Y. Blue-emissive upconversion nanoparticles for low-power-excited bioimaging in vivo. *J. Am. Chem. Soc.* **134,** 5390–5397 (2012).
54 Liu, Q., Yin, B. R., Yang, T. S., Yang, Y. C., Shen, Z., Yao, P. & Li, F. Y. A general strategy for biocompatible, high-effective upconversion nanocapsules based on triplet–triplet annihilation. *J. Am. Chem. Soc.* **135,** 5029–5037 (2013).
55 Bogdan, N., Vetrone, F., Ozin, G. A. & Capobianco, J. A. Synthesis of ligand-free colloidally stable water dispersible brightly luminescent lanthanide-doped upconverting nanoparticles. *Nano Lett.* **11,** 835–840 (2011).
56 Dong, A. G., Ye, X. C., Chen, J., Kang, Y. J., Gordon, T., Kikkawa, J. M. & Murray, C. B. A generalized ligand-exchange strategy enabling sequential surface functionalization of colloidal nanocrystals. *J. Am. Chem. Soc.* **133,** 998–1006 (2010).
57 Liu, Q., Sun, Y., Li, C. G., Zhou, J., Li, C. Y., Yang, T. S., Zhang, X. Z., Yi, T., Wu, D. M. & Li, F. Y. ^{18}F-Labeled magnetic-upconversion nanophosphors via rare-Earth cation-assisted ligand assembly. *ACS Nano* **5,** 3146–3157 (2011).
58 Cheng, L., Yang, K., Shao, M. W., Lu, X. H. & Liu, Z. In vivo pharmacokinetics, long-term biodistribution and toxicology study of functionalized upconversion nanoparticles in mice. *Nanomedicine* **6,** 1327–1340 (2011).
59 Kobayashi, H., Kosaka, N., Ogawa, M., Morgan, N. Y., Smith, P. D., Murray, C. B., Ye, X. C., Collins, J., Kumar, G. A., Bell, H. & Choyke, P. L. In vivo multiple color lymphatic imaging using upconverting nanocrystals. *J. Mater. Chem.* **19,** 6481–6484 (2009).
60 Cao, T. Y., Yang, Y., Gao, Y., Zhou, J., Li, Z. Q. & Li, F. Y. High-quality water-soluble and surface-functionalized upconversion nanocrystals as luminescent probes for bioimaging. *Biomaterials* **32,** 2959–2968 (2011).
61 Xiong, L. Q., Chen, Z. G., Yu, M. X., Li, F. Y., Liu, C. & Huang, C. H. Synthesis, characterization, and in vivo targeted imaging of amine-functionalized rare-earth up-converting nanophosphors. *Biomaterials* **30,** 5592–5600 (2009).
62 Xiong, L. Q., Chen, Z. G., Tian, Q. W., Cao, T. Y., Xu, C. J. & Li, F. Y. High contrast upconversion luminescence targeted imaging in vivo using peptide-labeled nanophosphors. *Anal. Chem.* **81,** 8687–8694 (2009).
63 Wang, M., Mi, C. C., Wang, W. X., Liu, C. H., Wu, Y. F., Xu, Z. R., Mao, C. B. & Xu, S. K. Immunolabeling and NIR-excited fluorescent imaging of HeLa cells by using $NaYF_4$:Yb,Er upconversion nanoparticles. *ACS Nano* **3,** 1580–1586 (2009).
64 Liu, Y., Chen, M., Cao, T. Y., Sun, Y., Li, C. Y., Liu, Q., Yang, T. S., Yao, L. M., Feng, W. & Li, F. Y. A cyanine-modified nanosystem for in vivo upconversion luminescence bioimaging of methylmercury. *J. Am. Chem. Soc.* **135,** 9869–9876 (2013).
65 Cheng, L., Yang, K., Zhang, S., Shao, M. W., Lee, S. T. & Liu, Z. Highly-sensitive multiplexed in vivo imaging using PEGylated upconversion nanoparticles. *Nano Res.* **3,** 722–732 (2010).
66 Sun, Y. Multifunctionalized Rare Earth Upconversion Nanophosphors for in Vivo Imaging. Doctoral thesis, Fudan Univ. (2012).
67 Cheng, L., Wang, C., Ma, X. X., Wang, Q. L., Cheng, Y., Wang, H., Li, Y. G. & Liu, Z. Multifunctional upconversion nanoparticles for dual-modal imaging-guided stem cell therapy under remote magnetic control. *Adv. Funct. Mater.* **23,** 272–280 (2013).

68 Zhao, L., Kutikov, A., Shen, J., Duan, C. Y., Song, J. & Han, G. Stem cell labeling using polyethylenimine conjugated α-$NaYbF_4$:Tm^{3+}/CaF_2 upconversion nanoparticles. *Theranostics* **3,** 249–257 (2013).
69 Chen, F., Bu, W., Zhang, S., Liu, J., Fan, W., Zhou, L., Peng, W. & Shi, J. Gd^{3+}-ion-doped upconversion nanoprobes: relaxivity mechanism probing and sensitivity optimization. *Adv. Funct. Mater.* **23,** 298–307 (2013).
70 Xia, A., Chen, M., Gao, Y., Wu, D. M., Feng, W. & Li, F. Y. Gd^{3+} complex-modified $NaLuF_4$-based upconversion nanophosphors for trimodality imaging of NIR-to-NIR upconversion luminescence, X-Ray computed tomography and magnetic resonance. *Biomaterials* **33,** 5394–5405 (2012).
71 Xia, A., Gao, Y., Zhou, J., Li, C. Y., Yang, T. S., Wu, D. M., Wu, L. M. & Li, F. Y. Core-shell $NaYF_4$:Yb^{3+},Tm^{3+}@Fe_xO_y nanocrystals for dual-modality T_2-enhanced magnetic resonance and NIR-to-NIR upconversion luminescent imaging of small-animal lymphatic node. *Biomaterials* **32,** 7200–7208 (2011).
72 Chen, F., Zhang, S. J., Bu, W. B., Liu, X. H., Chen, Y., He, Q. J., Zhu, M., Zhang, L. X., Zhou, L. P., Peng, W. J. & Shi, J. L. A "neck-formation" strategy for an antiquenching magnetic/upconversion fluorescent bimodal cancer probe. *Chem. Eur. J* **16,** 11254–11260 (2010).
73 Liu, Y. L., Ai, K. L., Liu, J. H., Yuan, Q. H., He, Y. Y. & Lu, L. H. A High-performance ytterbium-based nanoparticulate contrast agent for in vivo X-Ray computed tomography imaging. *Angew. Chem. Int. Ed.* **51,** 1437–1442 (2011).
74 Xiao, Q. F., Bu, W. B., Ren, Q. G., Zhang, S. J., Xing, H. Y., Chen, F., Li, M., Zheng, X. P., Hua, Y. Q. & Zhou, L. P. Radiopaque fluorescence-transparent TaO_x decorated upconversion nanophosphors for in vivo CT/MR/UCL trimodal imaging. *Biomaterials* **33,** 7530–7539 (2012).
75 Sun, Y., Liu, Q., Peng, J. J., Feng, W., Zhang, Y. J., Yang, P. Y. & Li, F. Y. Radioisotope post-labeling upconversion nanophosphors for in vivo quantitative tracking. *Biomaterials* **34,** 2289–2295 (2013).
76 Yang, Y., Sun, Y., Cao, T. Y., Peng, J. J., Liu, Y., Wu, Y. Q., Feng, W., Zhang, Y. J. & Li, F. Y. Hydrothermal synthesis of $NaLuF_4$:^{153}Sm,Yb,Tm nanoparticles and their application in dual-modality upconversion luminescence and SPECT bioimaging. *Biomaterials* **34,** 774–783 (2013).
77 Dong, B., Xu, S., Sun, J., Bi, S., Li, D., Bai, X., Wang, Y., Wang, L. P. & Song, H. W. Multifunctional $NaYF_4$: Yb^{3+},Er^{3+}@Ag core/shell nanocomposites: integration of upconversion imaging and photothermal therapy. *J. Mater. Chem.* **21,** 6193–6200 (2011).
78 Cheng, L., Yang, K., Li, Y. G., Zeng, X., Shao, M. W., Lee, S. T. & Liu, Z. Multifunctional nanoparticles for upconversion luminescence/MR multimodal imaging and magnetically targeted photothermal therapy. *Biomaterials* **33,** 2215–2222 (2012).
79 Kang, X. J., Cheng, Z. Y., Li, C. X., Yang, D. M., Shang, M. M., Ma, P. A., Li, G. G., Liu, N. & Lin, J. Core–shell structured up-conversion luminescent and mesoporous $NaYF_4$:Yb^{3+}/Er^{3+}@$nSiO_2$@$mSiO_2$ nanospheres as carriers for drug delivery. *J. Phys. Chem. C* **115,** 15801–15811 (2011).
80 Gai, S. L., Yang, P. P., Li, C. X., Wang, W. X., Dai, Y. L., Niu, N. & Lin, J. Synthesis of magnetic, up-conversion luminescent, and mesoporous core-shell-structured nanocomposites as drug carriers. *Adv. Funct. Mater.* **20,** 1166–1172 (2010).
81 Fan, W. P., Shen, B., Bu, W. B., Chen, F., Zhao, K. L., Zhang, S. J., Zhou, L. P., Peng, W. J., Xiao, Q. F., Xing, H. Y., Liu, J. N., Ni, D. L., He, Q. J. & Shi, J. L. Rattle-structured multifunctional nanotheranostics for synergetic chemo-/radiotherapy and simultaneous magnetic/luminescent dual-mode imaging. *J. Am. Chem. Soc.* **135,** 6494–6503 (2013).
82 Yan, B., Boyer, J. C., Branda, N. R. & Zhao, Y. Near-infrared light-triggered dissociation of block copolymer micelles using upconverting nanoparticles. *J. Am. Chem. Soc.* **133,** 19714–19717 (2011).
83 Liu, J. N., Bu, W. B., Pan, L. M. & Shi, J. L. NIR-triggered anticancer drug delivery by upconverting nanoparticles with integrated azobenzene-modified mesoporous silica. *Angew. Chem. Int. Ed.* **52,** 4375–4379 (2013).
84 Yang, Y. M., Shao, Q., Deng, R. R., Wang, C., Teng, X., Cheng, K., Cheng, Z., Huang, L., Liu, Z., Liu, X. G. & Xing, B. G. In vitro and in vivo uncaging and bioluminescence imaging by using photocaged upconversion nanoparticles. *Angew. Chem. Int. Ed.* **51,** 3125–3129 (2012).
85 Yang, Y. M., Liu, F., Liu, X. G. & Xing, B. G. NIR light controlled photorelease of siRNA and its targeted intracellular delivery based on upconversion nanoparticles. *Nanoscale* **5,** 231–238 (2013).
86 Jayakumar, M. K. G., Idris, N. M. & Zhang, Y. Remote activation of biomolecules in deep tissues using near-infrared-to-UV upconversion nanotransducers. *Proc. Natl Acad. Sci. USA* **109,** 8483–8488 (2012).
87 Chatterjee, D. K., Fong, L. S. & Zhang, Y. Nanoparticles in photodynamic therapy: an emerging paradigm. *Adv. Drug Delivery Rev.* **60,** 1627–1637 (2008).
88 Qian, H. S., Guo, H. C., Ho, P. C. L., Mahendran, R. & Zhang, Y. Mesoporous-silica-coated up-conversion fluorescent nanoparticles for photodynamic therapy. *Small* **5,** 2285–2290 (2009).
89 Qiao, X. F., Zhou, J. C., Xiao, J. W., Wang, Y. F., Sun, L. D. & Yan, C. H. Triple-functional core-shell structured upconversion luminescent nanoparticles covalently grafted by photosensitizer for luminescent, magnetic resonance imaging and photodynamic therapy in vitro. *Nanoscale* **4,** 4611–4623 (2012).
90 Idris, N. M., Gnanasammandhan, M. K., Zhang, J., Ho, P. C., Mahendran, R. & Zhang, Y. In vivo photodynamic therapy using upconversion nanoparticles as remote-controlled nanotransducers. *Nat. Med.* **18,** 1580–1585 (2012).
91 Wang, C., Tao, H. Q., Cheng, L. & Liu, Z. Near-infrared light induced in vivo photodynamic therapy of cancer based on upconversion nanoparticles. *Biomaterials* **32,** 6145–6154 (2011).
92 Park, Y. I., Kim, H. M., Kim, J. H., Moon, K. C., Yoo, B., Lee, K. T., Lee, N., Choi, Y., Park, W., Ling, D., Na, K., Moon, W. K., Choi, S. H., Park, H. S., Yoon, S.-Y., Suh, Y. D., Lee, S. H. & Hyeon, T. Theranostic probe based on lanthanide-doped nanoparticles for simultaneous in vivo dual-modal imaging and photodynamic therapy. *Adv. Mater.* **24,** 5755–5761 (2012).
93 Wang, C., Cheng, L., Liu, Y. M., Wang, X. J., Ma, X. X., Deng, Z. Y., Li, Y. G. & Liu, Z. Imaging-guided pH-sensitive photodynamic therapy using charge reversible upconversion nanoparticles under near-infrared light. *Adv. Funct. Mater.* **23,** 3077–3086 (2013).
94 Wang, Y. F., Liu, G. Y., Sun, L. D., Xiao, J. W., Zhou, J. C. & Yan, C. H. Nd^{3+}-sensitized upconversion nanophosphors: efficient in vivo bioimaging probes with minimized heating effect. *ACS Nano* **7,** 7200–7206 (2013).
95 Xie, X. J., Gao, N. Y., Deng, R. R., Sun, Q., Xu, Q. H. & Liu, X. G. Mechanistic investigation of photon upconversion in Nd^{3+}-sensitized core-shell nanoparticles. *J. Am. Chem. Soc.* **135,** 12608–12611 (2013).
96 Shen, J., Chen, G. Y., Vu, A.-M., Fan, W., Bilsel, O. S., Chang, C. C. & Han, G. Engineering the upconversion nanoparticle excitation wavelength: cascade sensitization of tri-doped upconversion colloidal nanoparticles at 800 nm. *Adv. Opt. Mater.* **1,** 644–650 (2013).

Dr Wei Feng received his BS and PhD degrees in chemistry from Peking University in 2004 and 2009, respectively. He subsequently worked as a postdoctoral researcher on the synthesis and applications of upconversion nanomaterials with Prof. Chun-Hua Yan at Peking University for two years. He is currently a lecturer in the Department of Chemistry at Fudan University. His research interests include the design and synthesis of luminescent nanomaterials with a focus on their biological applications.

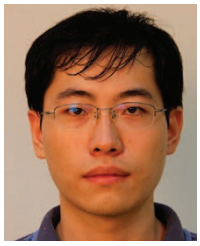

Xingjun Zhu was born in Shanghai, China, in 1990. He received his BS degree from Fudan University in 2012. Since then he has studied as an MS candidate under the guidance of Prof. Fuyou Li at Fudan University. His present research interests focus on the development of multifunctional upconversion nanomaterials for bioimaging and cancer therapy.

Prof. Fuyou Li was born in Zhejiang, China, in 1973 and received his PhD degree in 2000 from Beijing Normal University. He worked as a postdoctoral researcher at Peking University from 2000 to 2002, as an associate professor at Peking University from 2002 to 2003 and as an associate professor at Fudan University from 2003 to 2006. He has been working as a full professor at Fudan University since 2006. His current research interests include fluorescent probes, phosphorescent metal complexes and multifunctional rare-earth nanomaterials for sensing and bioimaging. To date, he has been an author or coauthor of over 150 scientific publications.